Electronic Supplementary Material (ESI) for Dalton Transactions.

Open and closed forms of the interpenetrated $[Cu_2(Tae)(Bpa)_2](NO_3)_2 \cdot nH_2O$ cationic coordination polymer: magnetic properties and high pressure CO_2/CH_4 gas sorption.

Roberto Fernández de Luis,[a] *Edurne S. Larrea,* [b] *Joseba Orive,*[c] *Arkaitz Fidalgo,* [a] *Luis Lezama,*[a,d] *María I. Arriortua.*[a,b]

[a]*BCMaterials (Basque Center for Materials, Applications & Nanostructures),Technological Park of Zamudio, Camino de Ibaizabal, Bndg. 500-1st, 48160, Derio, Spain.*

[b]*Departamento de Mineralogía y Petrología, Facultad de Ciencia y Tecnología, Universidad del País Vasco, UPV/EHU. 48940, Leioa, Spain.*

[c]*Departamento de Ciencia de Materiales, Facultad de Ciencias Físicas y Matemáticas (FCFM), Universidad de Chile. Av. Beauchef 851, Santiago, Chile*

[d]*Departamento de Química Inorgánica, Universidad del País Vasco, UPV/EHU. 48940, Leioa, Spain.*

roberto.fernandez@bcmaterials.net, edurne.serrano@ehu.eus, joseba.orive@ing.uchile.cl, arkaitz.fidalgo@bcmaterials.net; luis.lezama@ehu.eus, maribel.arriortua@ehu.eus

Table S1.- Crystallographic parameters for Closed$\cdot$5H_2O and Closed$\cdot$3.6H_2O compounds.

Closed 5H_2O					
Bond distances (Å)				Bond angles (º)	
C1-N2	1.355(6)	C8-C9	1.492(8)	O1-Cu1-O1^{ii}	92.3(2)
C1-C2	1.373(8)	N2-Cu1	2.004(4)	O1-Cu1-N2^{ii}	169.39(19)
C2-C3	1.378(9)	O1-Cu1	1.898(4)	O1^{ii}-Cu1-N2^{ii}	87.94(17)
C3-C4	1.379(8)	N1A-O1A	1.187(9)	O1-Cu1-N2	87.94(17)
C3-C6	1.509(8)	N1A-O2A	1.197(9)	O1^{ii}-Cu1-N2	169.40(19)
C4-C5	1.393(9)	N1A-O3A	1.206(9)	N2^{ii}-Cu1-N2	93.8(3)
C5-N2	1.319(8)	N2A-O5A	1.155(10)		
C6-C6^{i}	1.526(12)	N2A-O4A	1.160(9)	O1A-N1A-O2A	120.7(11)
C7-C8^{ii}	1.395(6)			O1A-N1A-O3A	120.0(11)
C7-C8	1.395(6)			O2A-N1A-O3A	118.7(10)
C7-C7^{iii}	1.505(12)			O5A-N2A-O4A^{iii}	127.2(15)
C8-O1	1.292(6)				
Closed 3.6H_2O					
Bond distances (Å)				Bond angles (º)	
C1-N2	1.346(10)	C8-O1	1.256(9)	O1-Cu1-O1^{ii}	91.8(3)
C1-C2	1.399(12)	C8-C9	1.518(11)	O1-Cu1-N2	88.2(2)
C2-C3	1.363(13)	N2-Cu1	1.987(6)	O1^{ii}-Cu1-N2	173.2(3)
C3-C4	1.412(12)	O1-Cu1	1.912(5)	N2-Cu1-N2^{ii}	92.6(4)
C3-C6	1.474 (12)	N2A-O1A	1.200(9)		
C4-C5	1.379(12)	N2A-O2A	1.199(9)		
C5-N2	1.354(10)	N2A-O3A	1.202(9)		
C6-C6^{i}	1.559(16)			O1A-N2A-O2A	120.9(10)
C7-C8	1.412(10)			O1A-N2A-O3A	119.4(10)
C7-C7^{iii}	1.470(20)			O2A-N2A-O3A	119.0(10)
Symmetry codes: (i) −*x*, −*y*+1, −*z*; (ii) −*x*+1/4, *y*, −*z*+1/4; (iii) −*x*+1/4, −*y*+1/4, *z*; (iv) −*x*−3/4, −*y*+1/4, *z*; (v) −*x*−3/4, *y*, −*z*+1/4; (vi) *x*, −*y*+1/4, −*z*+1/4.					

Figure S1.- Shape measurements. Location of the calculated distortion values for Closed·5H_2O and Closed·3.6H_2O in the shape maps for (a) six and (b) four coordination environments.

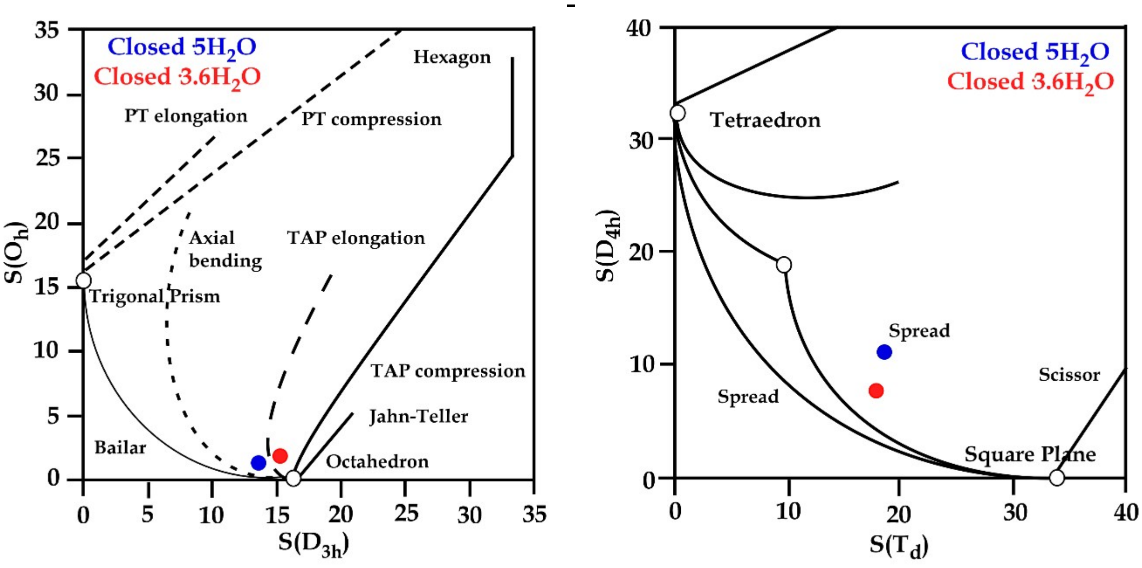

(a)

(b)

Figure S2.- Thermogravimetric and DSC curves for Closed 5H_2O and Open·2.4H_2O compounds.

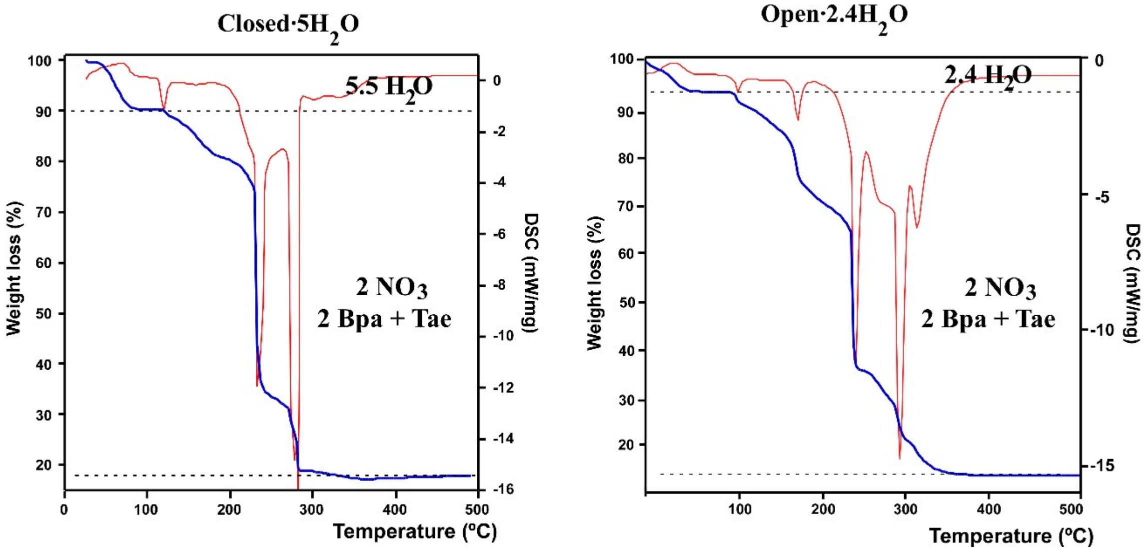

Figure S3.- Thermodiffractometry of Closed 5H_2O compound.

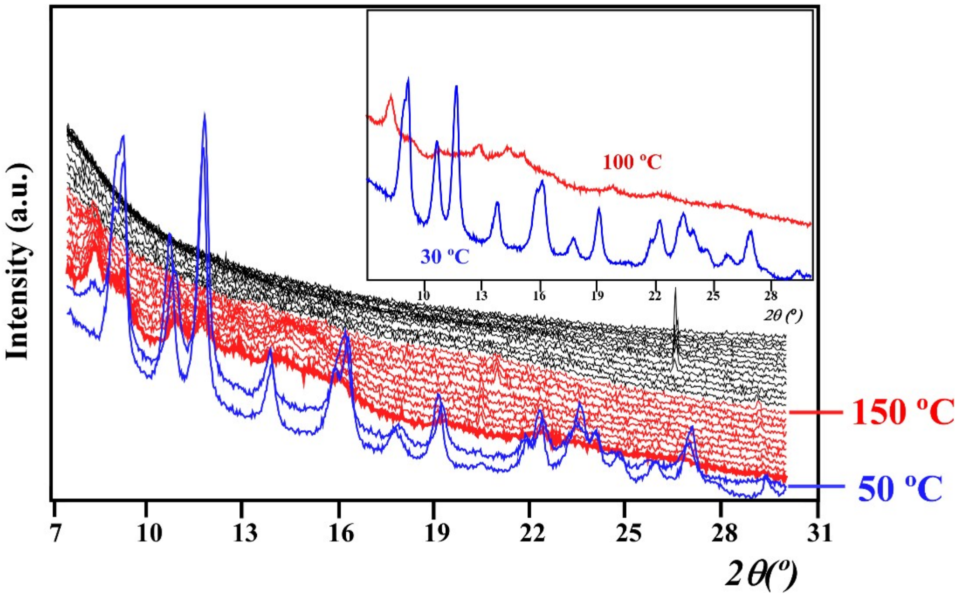

Figure S4.- X-ray diffraction patterns of the Open thermal activated structure (Open·An) after exposing to different solvents. Note that the Closed form of the crystal structure is recovered after the addition of the solvent.

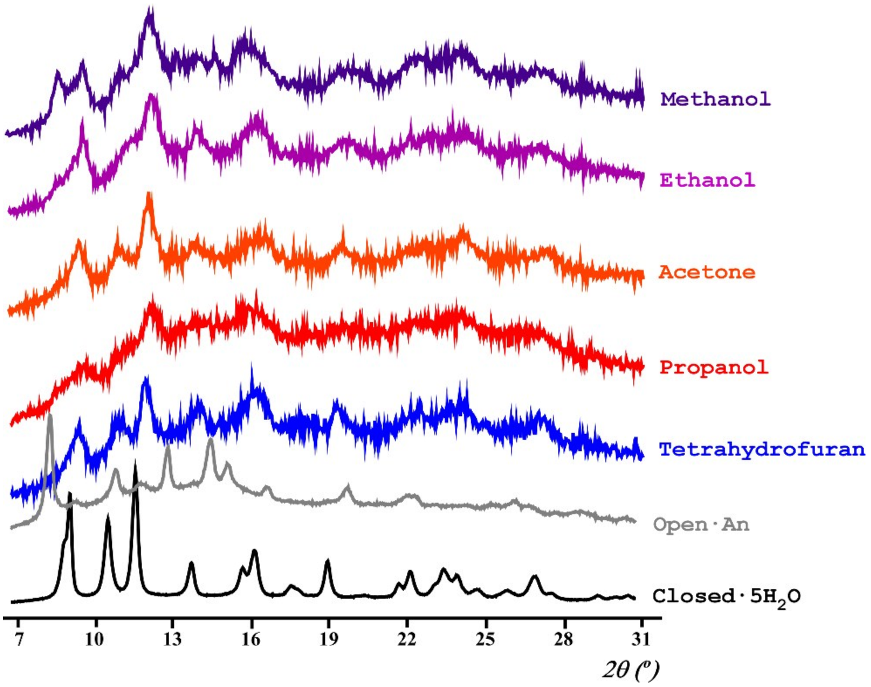

Figure S5.- Solid reflectance spectra of Closed·5H$_2$O and Open An compounds.

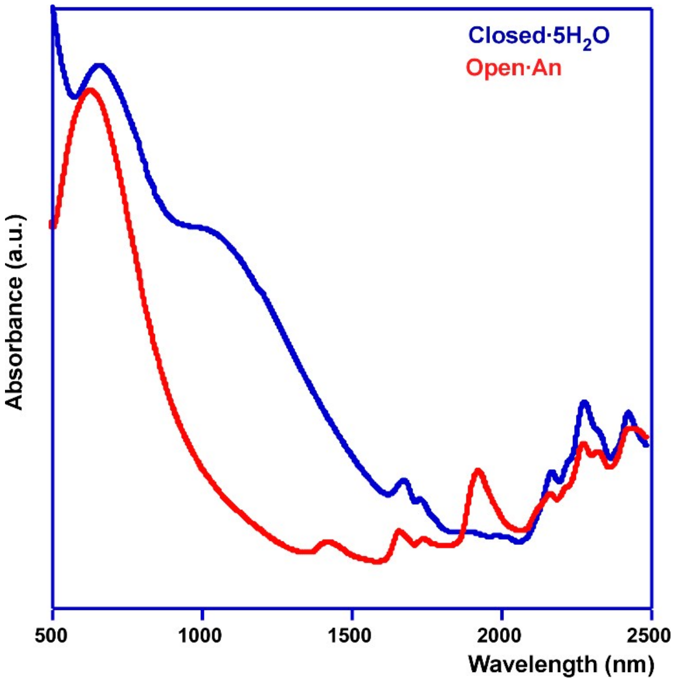

Figure S6.- Thermal evolution of two diffraction maxima of Open·2.4H_2O.

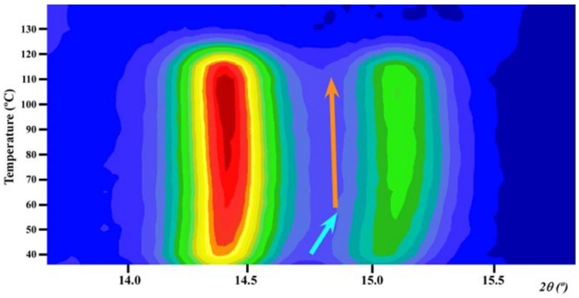

Figure S7.- Cell parameters and cell volume thermal evolution obtained from the peak fit of (040), (004) and (133) diffraction maxima of Open·2.4H_2O compound.

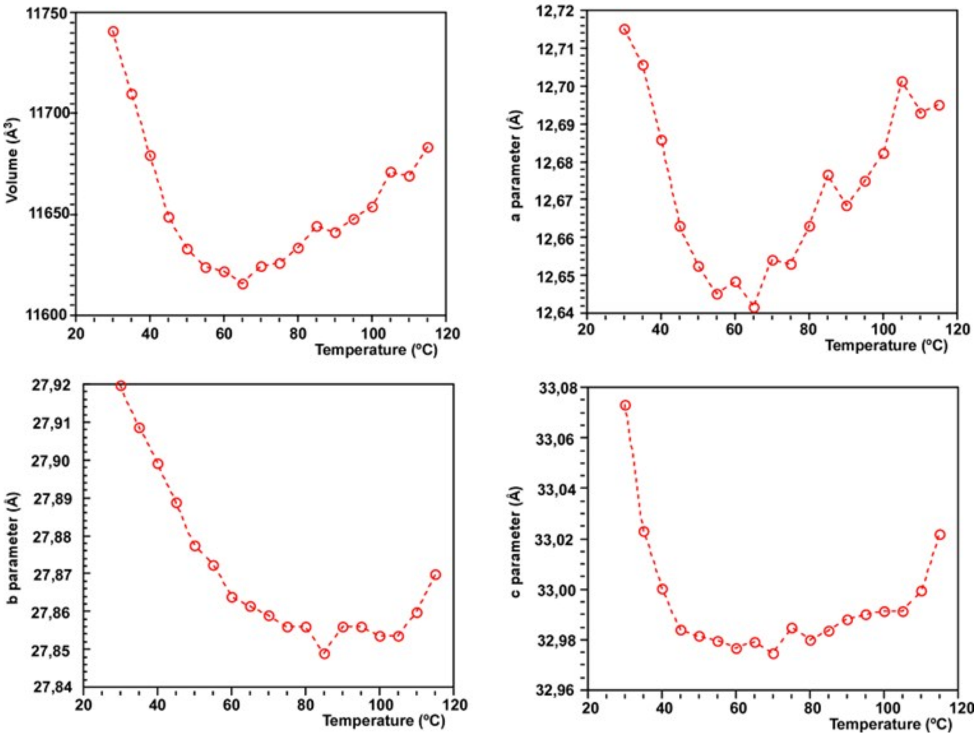

Figure S8.- χm and χmT curves for Open vacuum activated compound (from Closed·$5H_2O$)

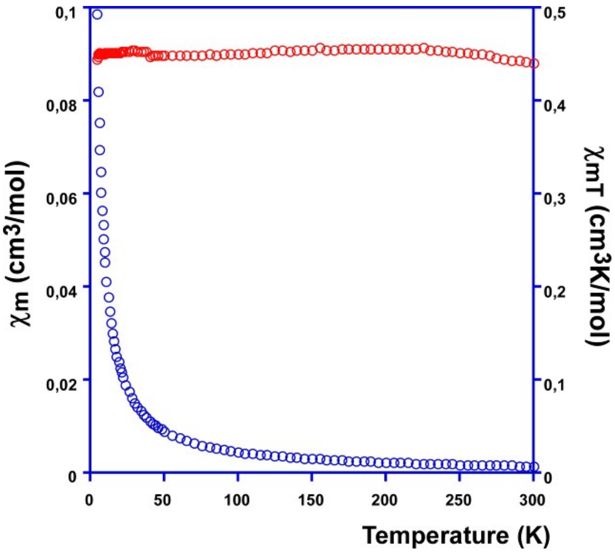

Figure S9.- (a) N_2 isotherm at 77K of Open·An. (b) CO_2/CH_4 selectivity at 15 and 30ºC at different pressures calculated by IAST method.

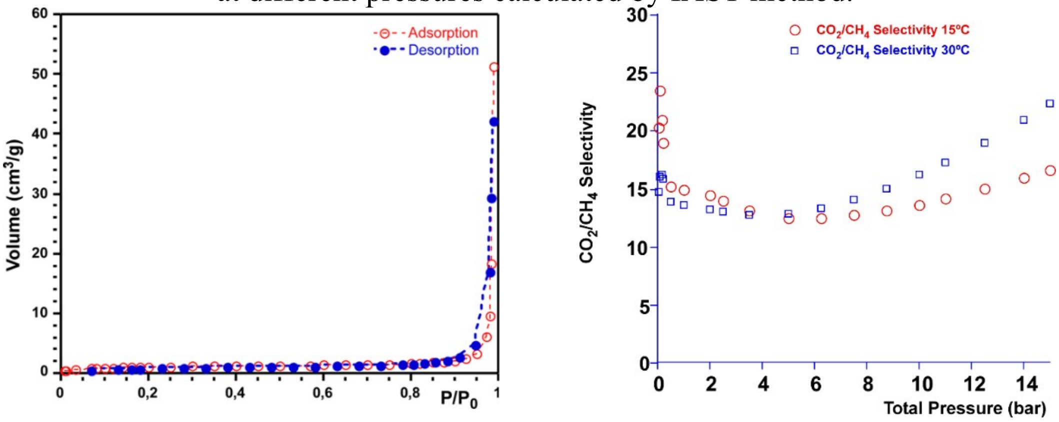

(a) (b)

Figure S10.- Van Hoff Plot for (a) CO_2 and (b) CH_4

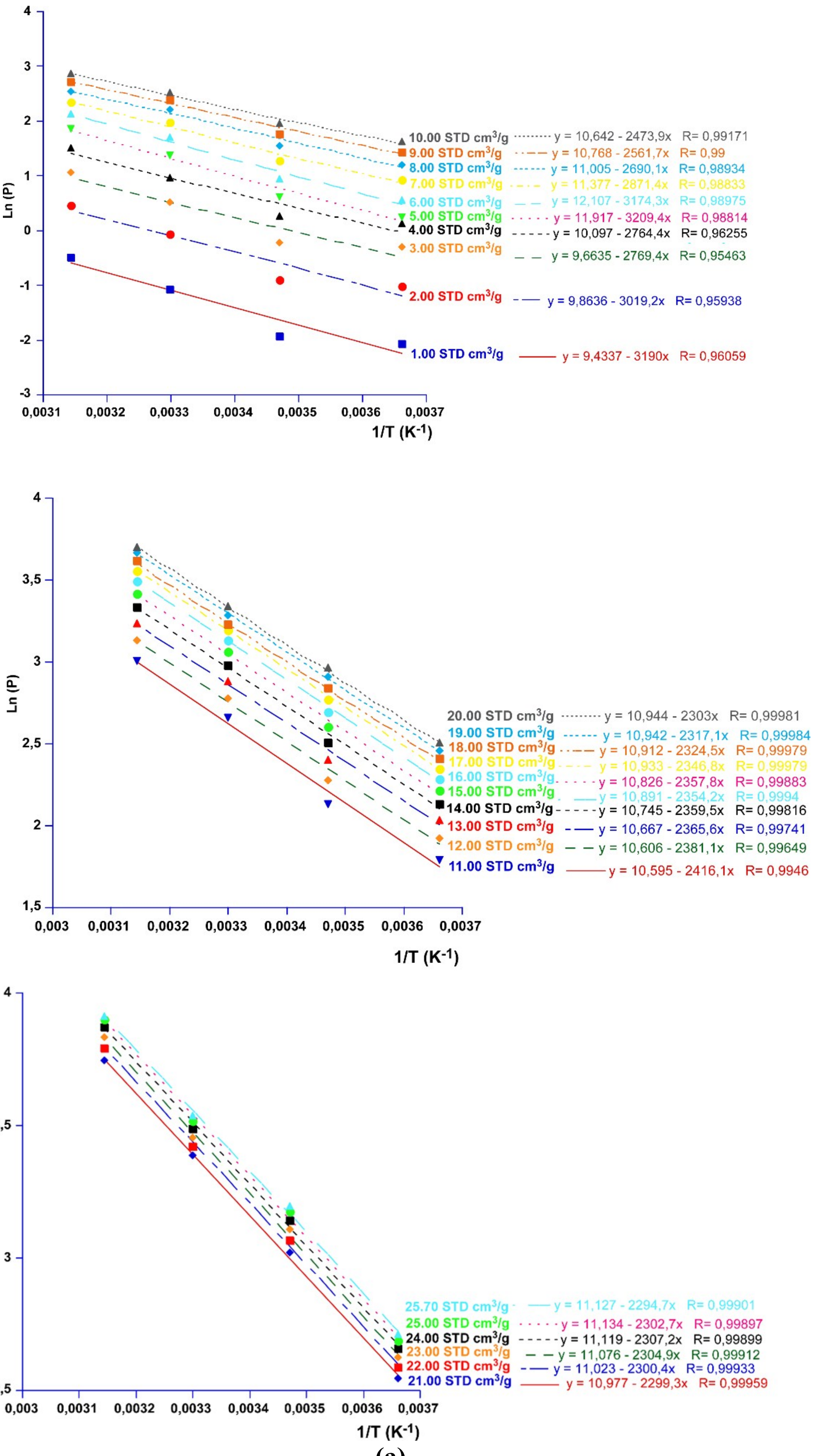

(a)

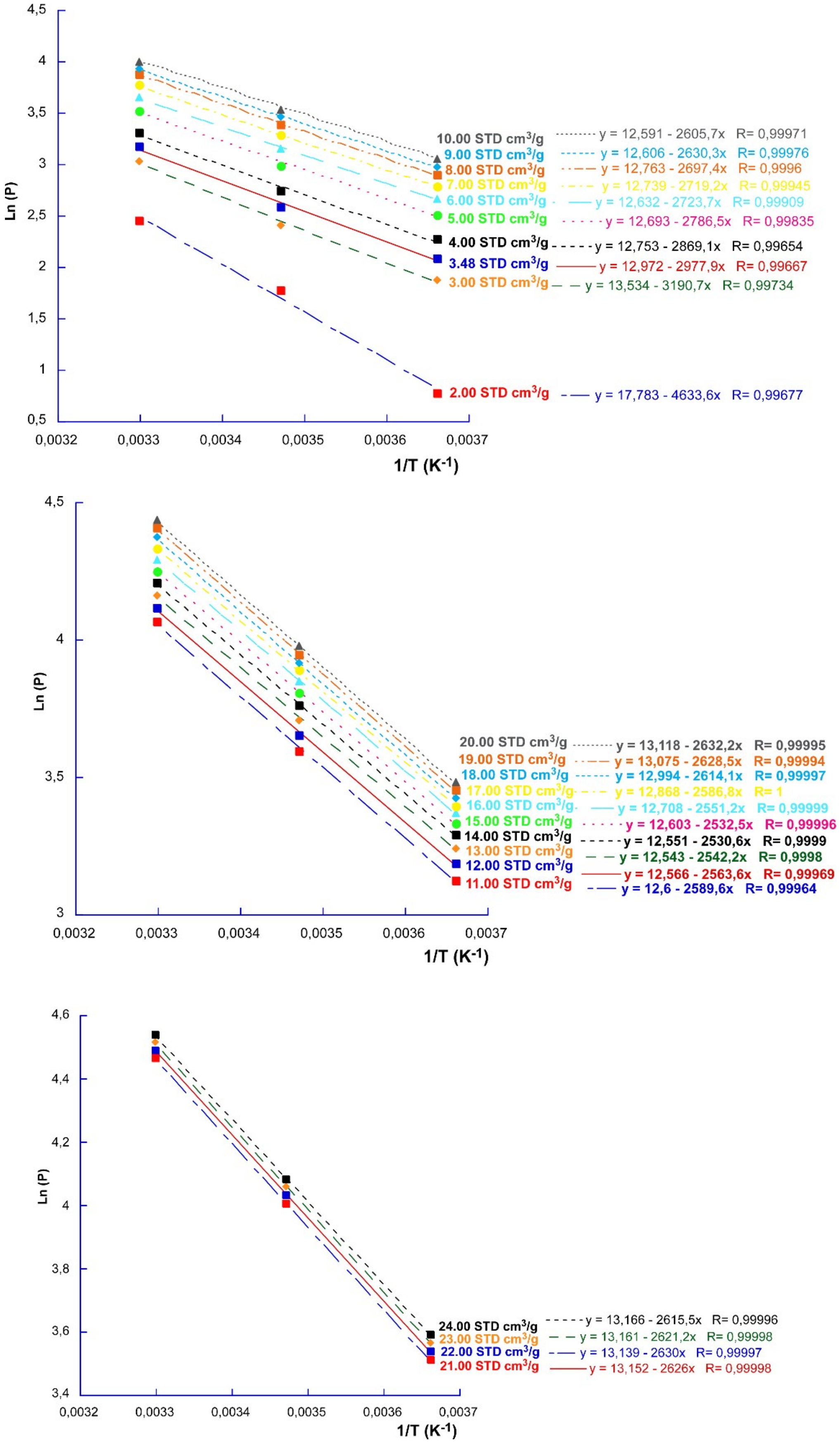
4,5
4
3,5
3
2,5
2
1,5
1
0,5
Ln (P)
0,0032
0,0033
0,0034
0,0035
0,0036
0,0037
1/T (K^{-1})
10.00 STD cm^3/g y = 12,591 - 2605,7x R= 0,99971
9.00 STD cm^3/g y = 12,606 - 2630,3x R= 0,99976
8.00 STD cm^3/g y = 12,763 - 2697,4x R= 0,9996
7.00 STD cm^3/g y = 12,739 - 2719,2x R= 0,99945
6.00 STD cm^3/g y = 12,632 - 2723,7x R= 0,99909
5.00 STD cm^3/g y = 12,693 - 2786,5x R= 0,99835
4.00 STD cm^3/g y = 12,753 - 2869,1x R= 0,99654
3.48 STD cm^3/g y = 12,972 - 2977,9x R= 0,99667
3.00 STD cm^3/g y = 13,534 - 3190,7x R= 0,99734
2.00 STD cm^3/g y = 17,783 - 4633,6x R= 0,99677
4,5
4
3,5
3
Ln (P)
0,0032
0,0033
0,0034
0,0035
0,0036
0,0037
1/T (K^{-1})
20.00 STD cm^3/g y = 13,118 - 2632,2x R= 0,99995
19.00 STD cm^3/g y = 13,075 - 2628,5x R= 0,99994
18.00 STD cm^3/g y = 12,994 - 2614,1x R= 0,99997
17.00 STD cm^3/g y = 12,868 - 2586,8x R= 1
16.00 STD cm^3/g y = 12,708 - 2551,2x R= 0,99999
15.00 STD cm^3/g y = 12,603 - 2532,5x R= 0,99996
14.00 STD cm^3/g y = 12,551 - 2530,6x R= 0,9999
13.00 STD cm^3/g y = 12,543 - 2542,2x R= 0,9998
12.00 STD cm^3/g y = 12,566 - 2563,6x R= 0,99969
11.00 STD cm^3/g y = 12,6 - 2589,6x R= 0,99964
4,6
4,4
4,2
4
3,8
3,6
3,4
Ln (P)
0,0032
0,0033
0,0034
0,0035
0,0036
0,0037
1/T (K^{-1})
24.00 STD cm^3/g y = 13,166 - 2615,5x R= 0,99996
23.00 STD cm^3/g y = 13,161 - 2621,2x R= 0,99998
22.00 STD cm^3/g y = 13,139 - 2630x R= 0,99997
21.00 STD cm^3/g y = 13,152 - 2626x R= 0,99998

(b)

Figure S11.- (a) Simulated diffraction patterns for Closed $5H_2O$ and Closed·$3.6H_2O$ compounds. (b) Experimental XRDP for samples synthesized at different conditions.

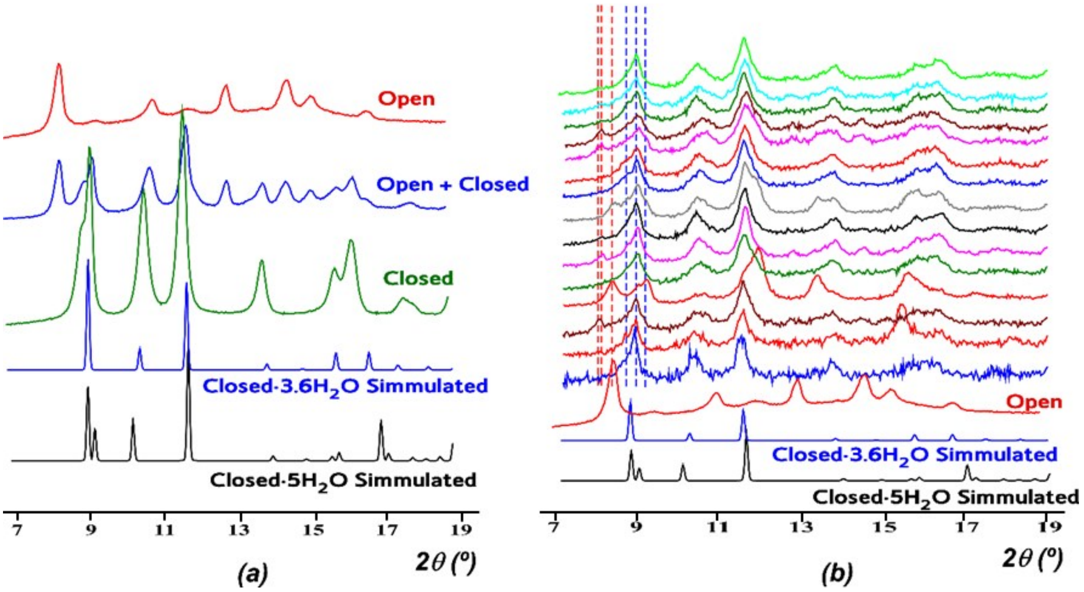

The differences between the simulated powder X-ray diffraction patterns are minimum, with a slight splitting of the reflections in the first diffraction maxima of Closed·$5H_2O$ compound. Nevertheless, if the medium half-width of the diffraction maxima is increased in the pattern simulation, this information is lost, as is observed in the experimental diffraction patterns. Examples of diffraction patterns for Closed, Open+Closed and Open phases are shown in FigS11 (a).

In FigS11 (b) different experimental patterns for samples synthesized in different conditions have been plotted. The crystallization of the closed and open forms of the compounds depends on the synthesis conditions, and in a wide range of conditions their co-crystallization is observed, as reflects the presence of two diffraction maxima between 8-10 º in 2θ(º). However, more interesting is the displacements observed for these two diffraction maxima. Depending on the synthesis conditions, the position of the first diffraction maxima for the closed and open phases is not exactly the same. This fact is highlighted with the dashed vertical lines in the FigS11 (b). The red dashed line stands for the different positions of the first diffraction maxima for the Open form compound, while the blue dashed line reflect the position of the first diffraction maxima of the Closed form of the compound. The great dispersion of the first maxima position for Closed and Open forms of the studied compounds is indicative of different degrees of interpenetrated metal organic nets openings probably related with the solvent content of the phases, and the disposition of the guess molecules within the pores, depending on the synthesis conditions.

Despite we have tried to differentiate the Closed·$5H_2O$ and Closed $3.6H_2O$ phases by powder X-ray diffraction, the broad half width of the diffraction maxima hinders the differentiation of the phases. Taking into account the small differences in the simulated diffraction patterns, and the experimental data, it is not possible to discern between both phases by lab-X-ray diffraction data.

Nevertheless, the experimental conditions for the crystallization of Closed·$5H_2O$ phase have been reported; because the thermal studies carried out in the samples obtained at this conditions indicate the presence of $5H_2O$ per formula unit.